Processing and Application of Ceramics 9 [1] (2015) 11–15
DOI: 10.2298/PAC1501011H

Magnetocaloric effect in Sr_2FeMoO_6/Ag composites

Mahmoud A. Hamad[1,2,*]

[1]*Physics Department, Faculty of Science, Tanta University, Egypt*
[2]*Physics Department, College of Science, Al Jouf University, Al Jouf, Skaka, P.O. Box 2014, Saudi Arabia*

Received 5 January 2015; Received in revised form 28 January 2015; Accepted 25 February 2015

Abstract

The enhanced low-field magnetocaloric effect was investigated for double perovskite Sr_2FeMoO_6 - silver (SFMO/Ag) composites with 0, 5 and 10 wt.% of Ag. A phenomenological model was used to predict magnetocaloric properties of SFMO/Ag composites, such as magnetic entropy change, heat capacity change and relative cooling power. It was shown that magnetic entropy change (ΔS_M) peaks of SFMO/Ag span over a wide temperature region, which can significantly improve the global efficiency of the magnetic refrigeration. Furthermore, the ΔS_M distribution of the SFMO/Ag composites is much more uniform than that of gadolinium. Through these results, SFMO/Ag composite has some potential application for magnetic refrigerants in an extended high-temperature range.

Keywords: *Sr_2FeMoO_6/Ag composites, magnetocaloric effect, modelling*

I. Introduction

Modern cooling offers a green solution to this emerging challenge and it allows to generate both heating and cooling. The modern cooling technology is based on the use of the magnetocaloric effect (MCE) or electrocaloric effect. It offers a green solution to refrigerant fluids such as chlorofluorocarbons, hydrochlorofluorocarbons and ammonia based compounds. Furthermore, the intrinsic better performance is the reason that this cooling system reduces the electric energy used to run refrigeration units [1–14]. The magnetic cooling technology is based on the use of the magnetocaloric effect applied to various metallic materials and new alloys named magnetocaloric materials. Magnetization/demagnetization cycles are then similar to compression/ expansion of a gas and can be used for cooling [15,16]. In principle, magnetic refrigeration is based on the magnetocaloric effect, which is the temperature change of a magnetic material associated with an external magnetic field change in an adiabatic process. The applications of the magnetic properties of magnetic materials become more and more significant for the reliability [17–19]. Double perovskite Sr_2FeMoO_6 (SFMO) is a very important material having high potential for spintronic and magnetoresistive applications. It is half-metallic resulting in 100% spin polarized charge carriers and it has one of the highest Curie temperatures, T_c, among half metals, around 410–450 K [20–23].

In this paper, the enhanced low-field magnetocaloric effect is investigated for Sr_2FeMoO_6/Ag (SFMO/Ag) composite samples with 0, 5 and 10 wt.% of Ag. A phenomenological model was used to predict magnetocaloric properties of SFMO/Ag such as magnetic entropy change, heat capacity change and relative cooling power.

II. Theoretical Considerations

According to the phenomenological model, proposed by Hamad [24], the dependence of magnetization on variation of temperature and Curie temperature T_c is presented by:

$$M = \frac{M_i - M_f}{2} \tanh\left(A\left(T_c - T\right)\right) + B \cdot T + C \qquad (1)$$

where M_i is an initial value of magnetization at ferromagnetic-paramagnetic transition and M_f is a final value of magnetization at ferromagnetic-paramagnetic transition as shown in Fig. 1. The parameters A and C are expressed by the following two equations:

$$A = \frac{2(B - S_c)}{M_i - M_f} \qquad (2)$$

*Corresponding author: tel: +966 530714921
e-mail: *m_hamad76@yahoo.com*

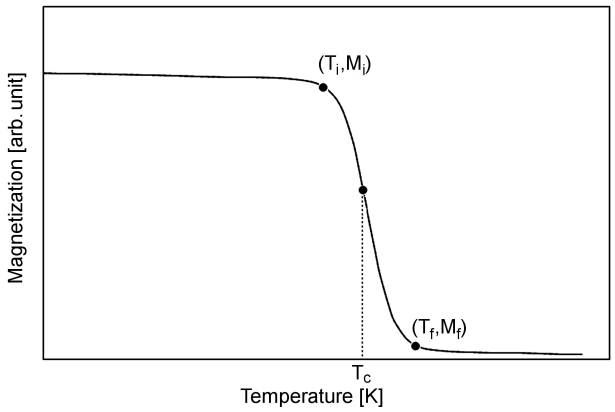

Figure 1. Temperature dependence of magnetization in constant applied magnetic field

$$C = \frac{M_i + M_f}{2} - B \cdot T_c \tag{3}$$

where B is magnetization sensitivity $\mathrm{d}M/\mathrm{d}T$ at ferromagnetic state before transition and S_c is magnetization sensitivity $\mathrm{d}M/\mathrm{d}T$ at Curie temperature T_c.

A magnetic entropy change of a magnetic system under adiabatic magnetic field variation from 0 to final value H_{max} is available by:

$$\Delta S_M = \left(-A\frac{M_i - M_f}{2}\,\mathrm{sech}^2(A(T_c - T)) + B\right)H_{max} \tag{4}$$

The observed relatively large magnetic entropy change is attributed to high magnetic moment and rapid change of magnetization at T_c. Thus, maximal magnetic entropy change ΔS_{max} can be evaluated from equation (4) for $T_c = T$ by the following equation:

$$\Delta S_{max} = H_{max}\left(-A\frac{M_i - M_f}{2} + B\right) \tag{5}$$

In addition, determination of full-width at half-maximum of magnetic entropy change, δT_{FWHM}, can be carried out as follows:

$$\delta T_{FWHM} = \frac{2}{A}\cosh^{-1}\left(\sqrt{\frac{2A(M_i - M_f)}{A(M_i - M_F) + 2B}}\right) \tag{6}$$

Full-width at half-maximum is important for estimation of magnetic cooling efficiency. A magnetic cooling efficiency is estimated by considering magnitude of magnetic entropy change (ΔS_M) and its full-width at half-maximum (δT_{FWHM}) [25]. A product of $-\Delta S_{max}$ and δT_{FWHM} is called relative cooling power (*RCP*) based on magnetic entropy change and can be calculated by:

$$RCP = -\Delta S_M(T, H_{max}) \times \left(M_i - M_f - 2\frac{B}{A}\right)H_{max} \times \\ \times \cosh^{-1}\left(\sqrt{\frac{2A(M_i - M_f)}{A(M_i - M_F) + 2B}}\right) \tag{7}$$

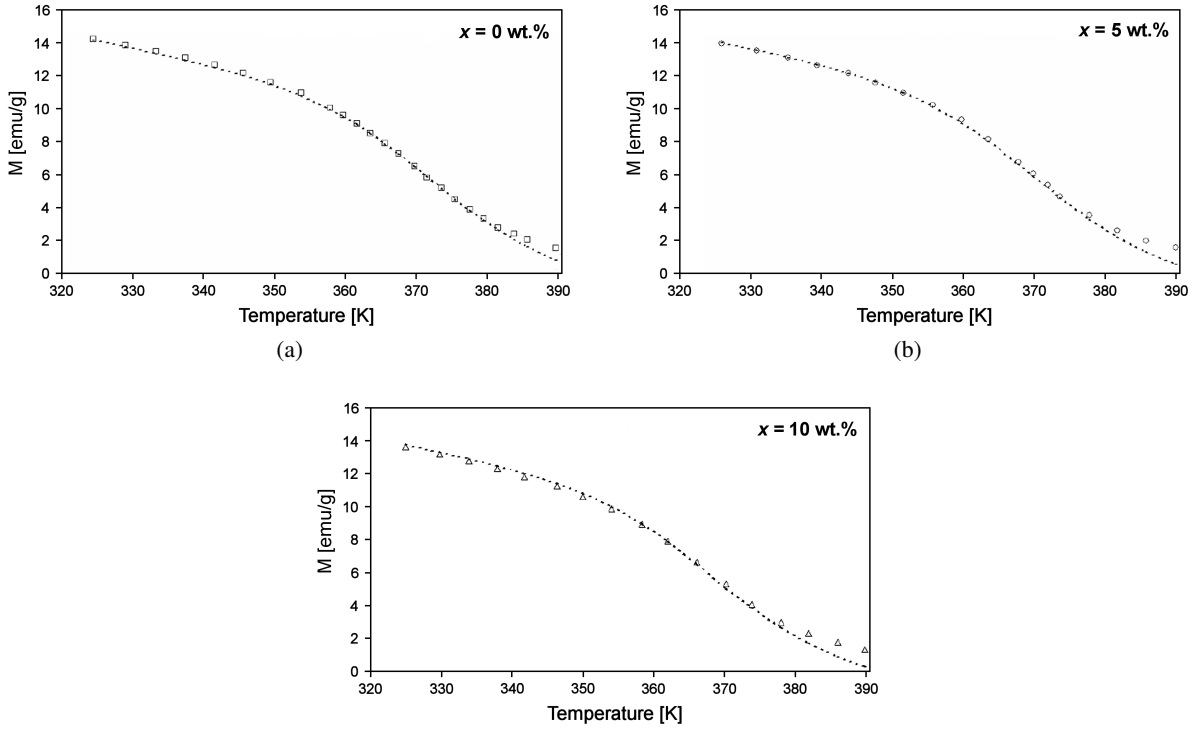

Figure 2. Magnetization in 0.1 T magnetic field for the SFMO/Ag versus temperature. The dashed curves are modelled results and symbols represent experimental data from Ref. 26

Table 1. Model parameters for SFMO/Ag in 0.1 T applied magnetic field

x [wt.%]	M_i [emu/g]	M_f [emu/g]	T_c [K]	B [emu/g·K]	S_c [emu/g·K]
0	10.2	1.7	372	-0.088	-0.35
5	10.2	1.7	370	-0.088	-0.35
10	10.01	1.7	368	-0.088	-0.35

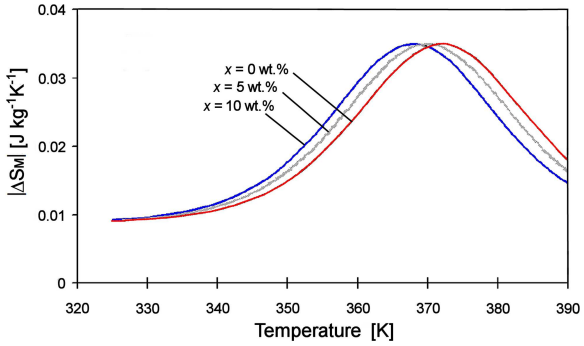

Figure 3. Magnetic entropy change as function of temperature for SFMO/Ag in 0.1 T magnetic field change

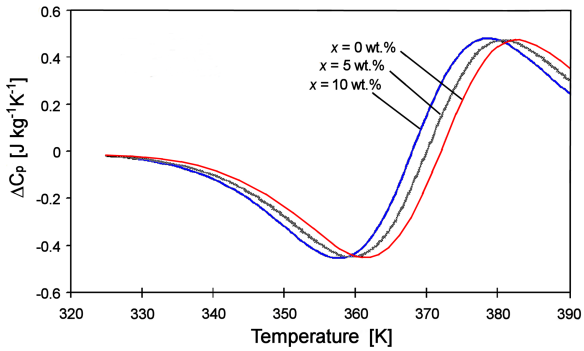

Figure 4. Heat capacity change as function of temperature for SFMO/Ag in 0.1 T magnetic field change

The magnetization-related change of the specific heat is given by [25]:

$$\Delta C_{P,H} = T\frac{\delta \Delta S_M}{\delta T} \tag{8}$$

According to this model heat capacity change, $\Delta C_{P,H}$, can be expressed as [24]:

$$\Delta C_{P,H} = -TA^2(M_i - M_f)\,\mathrm{sech}^2(A(T_c - T))\cdot \tanh(A(T_c - T))H_{max} \tag{9}$$

From this phenomenological model, δT_{FWHM}, $|\Delta S|_{max}$, RCP and ΔT can be simply evaluated for SFMO/Ag composite samples under magnetic field variation.

III. Results and discussion

Figure 2 shows magnetization versus temperature in 0.1 T magnetic field for SFMO + xAg (x = 0, 5 and 10 wt.%) composite samples. The symbols represent experimental data from literature [26], while the dashed curves represent modelled data obtained by using model parameters given in Table 1. These parameters were determined from experimental data. Figures 3 and 4 show predicted values for change of magnetic entropy and heat capacity as functions of temperature, respectively. It is obvious that magnetic entropy change (ΔS_M) peaks of SFMO/Ag span over a wide temperature region. It is also clear that ΔS_{max} of SFMO/Ag does not change considerably with increasing Ag concentration. This is due to the Ag distribution on the grain boundaries of SFMO instead of incorporation of Ag in the SFMO structure.

It is well reported for manganites that Ag cannot substitute the rare-earth cations, but might segregates at the grain surface/boundaries [27,28]. There is a large difference between the ionic radius of Ag^+ (1.15 Å) and that of transition metal ions, Fe^{3+} (0.65 Å) and Mo^{5+} (0.61 Å), which prevents substitution and favours Ag segregating at grain boundaries according to the Hume-Rothery criteria. X-ray diffraction patterns of the SFMO/Ag composites [26] confirmed that the metallic Ag does not enter into the lattice of SFMO and no change in the lattice parameter was observed. Moreover, the results presented by Kumar *et al.* [26] indicated that small Ag particles are randomly distributed over the SFMO grains indicating that no chemical reaction occurs between SFMO and Ag particles. The distribution of Ag particles, noticed on the peripheries of the SFMO grains, was found to increase with the increase in Ag content. Furthermore, the high resolution field emission scanning electron microscope measurements showed that no apparent variations in morphology and particle size are observed in spite of the existence of Ag particles over the surface of SFMO grains [26]. Thus, SFMO and Ag form two phase composite system, in which the Ag metal phase occurs in the form of the secondary phase. Therefore, it may be concluded that Ag remains mainly at the grain surface/boundary of SFMO grains in these composites.

It was also shown by Kumar *et al.* [26] that the resistivity and saturation magnetization slightly decrease with the increase of the Ag content in the composite samples. The decrement in value of magneto-resistance is due to the presence of metallic Ag at the grain surface/boundaries of SFMO, which suppress the spin polarized tunnelling and reduces the magneto-resistance.

The values of maximum magnetic entropy change, full-width at half maximum and relative cooling power of the SFMO/Ag composite samples made with different plating times, in 0.1 T magnetic field variation, were calculated by equations (5), (6) and (7), respectively, and tabulated in Table 2. Furthermore, the maximum

Table 2. The predicted values of magnetocaloric properties for SFMO/Ag in 0.1 T applied magnetic field

Composition	ΔH [T]	$-\Delta S_{max}$ [J/kg·K]	δT_{FWHM} [K]	RCP [J/kg]	$\Delta C_{P,H(max)}$ [J/kg·K]	$\Delta C_{P,H(min)}$ [J/kg·K]
SFMO	0.1	0.03	37.26	1.3	0.48	-0.45
SFMO / 5 wt.% Ag	0.1	0.03	37.26	1.3	0.47	-0.44
SFMO / 10 wt.% Ag	0.1	0.03	36.43	1.27	0.48	-0.45

Table 3. The predicted values of magnetocaloric properties for some compositions in low applied magnetic field changes

Composition	ΔH [T]	$-\Delta S_{max}$ [J/kg·K]	δT_{FWHM} [K]	RCP [J/kg]	$\Delta C_{P,H(max)}$ [J/kg·K]	$\Delta C_{P,H(min)}$ [J/kg·K]	Ref.
$Ge_{0.95}Mn_{0.05}$ film	0.1	(0.4–3.6)10^{-6}	12.69–17.75	(0.63–0.45)10^{-5}	(0.077–1.1)10^{-4}	-(0.073–1)10^{-4}	[39]
$La_{1-x}Cd_xMnO_3$	0.05	0.011	29.65–44.03	0.326–0.484	0.087–0.105	-(0.07–0.094)	[40]
$Gd_{1-x}Ca_xBaCo_2O_{5.5}$	0.1	(1.65–2.2)10^{-6}	9.77–13.85	(1.61–3.04)10^{-5}	(6.14–6.34)10^{-5}	-(6.94–6.13)10^{-5}	[41]

and minimum values of specific heat change for each sample were determined from Fig. 4. The calculated values of ΔS_M (Table 2) suggest that SFMO/Ag composite is a promising candidate for magnetocaloric materials. Moreover, the large temperature width of the ΔS_M peak is advantageous for practical application, which can significantly improve the global efficiency of the magnetic refrigeration. Therefore, this is a feature for its use as a magnetocaloric material in a real cooling device. Furthermore, the ΔS_M distribution of the SFMO/Ag composite is much more uniform than that of gadolinium [29,30]. This feature is desirable for an Ericson-cycle magnetic refrigerator [31]. In addition, perovskite like structured materials are easier to fabricate and possess a higher chemical stability. The magnetic entropy change in perovskite manganites could be attributed to the considerable variation of the magnetization near T_c [32].

The spin-lattice coupling in the magnetic ordering process could play a considerable role in additional magnetic entropy change [33]. Due to strong coupling between spin and lattice, significant lattice change accompanying magnetic transition in perovskite manganites has been observed [34,35]. This coupling mechanism induces the lattice structural change, which induces a volume variation and thus can cause an additional change in magnetism. Thereby, a greater reduction of magnetization near T_c occurs and results in significant magnetic entropy change [36–38]. In this way, a conclusion might be drawn that a strong spin-lattice coupling in the magnetic transition process would lead to additional magnetic entropy change near T_c, and consequently, favours the magnetocaloric effect. Table 3 shows the predicted values of magnetocaloric properties for some other compositions in low applied magnetic field change (ΔH). The magnetocaloric properties of SFMO/Ag composite are significantly better than that of $Ge_{0.95}Mn_{0.05}$, $La_{1-x}Cd_xMnO_3$ and $Gd_{1-x}Ca_xBaCo_2O_{5.5}$ as shown in Tables 2 and 3 [39–41].

IV. Conclusions

A phenomenological model was used to predict magnetocaloric properties of SFMO/Ag composites, such as magnetic entropy change, heat capacity change and relative cooling power. It is shown that SFMO/Ag composite samples have magnetic entropy change (ΔS_M) peaks spanning over a wide temperature region. ΔS_M distribution is uniform, which is desirable for Ericsson-cycle magnetic refrigerator. In addition, these samples have higher chemical stability. Moreover, the results point out the SFMO/Ag composite samples are excellent candidates as working materials for magnetic refrigerants at high temperatures.

References

1. M.A. Hamad, "Magnetocaloric effect in $La_{1.25}Sr_{0.75}MnCoO_6$", *J. Therm. Anal. Calorim.*, **115** (2014) 523–526.
2. M.A. Hamad, "Lanthanum concentration effect of magnetocaloric properties in $La_xMnO_{3-\delta}$", *J. Supercond. Nov. Magn.*, **28** (2015) 173–178.
3. M.A. Hamad, "Giant electrocaloric properties of relaxor ferroelectric 0.93PMN-0.07PT thin film at room temperature", *AIP Advances*, **3** (2013) 032115.
4. M.A. Hamad, "Giant isothermal entropy change in (111)-oriented PMN-PT thin film", *J. Adv. Dielectrics*, **4** (2014) 1450026.
5. M.A. Hamad, "Magnetocaloric effect in $La_{0.65-x}Eu_xSr_{0.35}MnO_3$", *Phase Transitions*, **87** (2014) 460–467.
6. M.A. Hamad, "Electrocaloric properties of Zr-modified $Pb(Mg_{1/3}Nb_{2/3})O_3$ polycrystalline ceramics", *J. Adv. Dielectrics*, **3** (2013) 1350029.
7. M.A. Hamad, "Magnetocaloric effect in nanopowders of $Pr_{0.67}Ca_{0.33}Fe_xMn_{1-x}O_3$", *J. Supercond. Nov. Magn.*, **27** (2014) 223–227.
8. M.A. Hamad, "Magnetocaloric effect of perovskite $Eu_{0.5}Sr_{0.5}CoO_3$", *J. Supercond. Nov. Magn.*, **27** (2014) 277–280.
9. M.A. Hamad, "Magnetocaloric effect in $La_{0.7}Sr_{0.3}MnO_3/Ta_2O_5$ composites", *J. Adv. Ceram.*, **2** (2013) 213–217.
10. M.A. Hamad, "Theoretical investigations on electrocaloric properties of $PbZr_{0.95}Ti_{0.05}O_3$ thin film", *Int. J. Thermophys.*, **34** (2013) 1158–1165.

11. A. Chaturvedi, S. Stefanoski, M.H. Phan, G.S. Nolas, H. Srikanth, "Table-like magnetocaloric effect and enhanced refrigerant capacity in $Eu_8Ga_{16}Ge_{30}$-EuO composite materials", *Appl. Phys. Lett.*, **99** (2011) 162513.
12. M.A. Hamad, "Detecting giant electrocaloric properties of ferroelectric SbSI at room temperature", *J. Adv. Dielectrics*, **3** (2013) 1350008.
13. M.A. Hamad, "Magnetocaloric effect in half-metallic double perovskite $Sr_{0.4}Ba_{1.6-x}Sr_xFeMoO_6$", *Int. J. Thermophys.*, **34** (2013) 2144–2151.
14. M.A. Hamad, "Magnetocaloric effect in (001)-oriented MnAs thin film", *J. Supercond. Nov. Magn.*, **27** (2014) 263–267.
15. M.A. Hamad, "Magnetocaloric effect of perovskite manganites $Ce_{0.67}Sr_{0.33}MnO_3$", *J. Supercond. Nov. Magn.*, **26** (2013) 2981–2984.
16. M.A. Hamad, "Simulation of magnetocaloric effect in $La_{0.7}Ca_{0.3}MnO_3$ ceramics fabricated by fast sintering process", *J. Supercond. Nov. Magn.*, **27** (2014) 269–272.
17. M.A. Hamad, "Ni-Co-Mo-Ti maraging steel hysteretic loops calculations", *Mater. Sci. Eng. R, Arab. J. Sci. Eng.*, **39** (2014) 569–574.
18. M.A. Hamad, "Prediction of energy loss of $Ni_{0.58}Zn_{0.42}Fe_2O_4$ nanocrystalline and Fe_3O_4 nanowire arrays", *Jpn. J. Appl. Phys.*, **49** (2010) 085004.
19. M.A. Hamad, "Calculations on nanocrystalline $CoFe_2O_4$ prepared by polymeric precursor method", *J. Supercond. Nov. Magn.*, **26** (2013) 669–673.
20. K.I. Kobayashi, T. Kimura, H. Sawada, K. Terakura, Y. Tokura, "Room-temperature magnetoresistance in an oxide material with an ordered double-perovskite structure", *Nature*, **395** (1998) 677–680.
21. D.D. Sarma, P. Mahadevan, T. Saha-Dasgupta, S. Ray, A. Kumar, "Electronic structure of Sr_2FeMoO_6", *Phys. Rev. Lett.*, **85** (2000) 2549–2552.
22. J. Rager, A.V. Berenov, L.F. Cohen, W.R. Branford, Y.V. Bugoslavsky, Y. Miyoshi, M. Ardakani, J.L. MacManus-Driscoll, "Highly aligned, spin polarized thin films of Sr_2FeMoO_6 by a chemical vapor process", *Appl. Phys. Lett.*, **81** (2002) 5003.
23. C.L. Yuan, Y. Zhu, P.P. Ong, C.K. Ong, T. Yu, Z.X. Shen, "Grain boundary effects on the magnetotransport properties of Sr_2FeMoO_6 induced by variation of the ambient H_2-Ar mixture ratio during annealing", *Physica B*, **334** (2003) 408–412.
24. M.A. Hamad, "Magnetocaloric effect in $Sr_{0.4}Ba_{1.6-x}La_xFeMoO_6$", *J. Supercond. Nov. Magn.*, **27** (2014) 1777–1780.
25. M.A. Hamad, "Simulation of magnetocaloric properties of antiperovskite structural $Ga_{1-x}Al_xCMn_3$", *J. Supercond. Nov. Magn.*, **27** (2014) 2569–2572.
26. N. Kumar, R.P. Aloysius, A. Gaur, R.K. Kotnala, "Study of ferromagnetic-metal type Sr_2FeMoO_6 + xAg (x=0–10 wt%) composites", *J. Alloys Compd.*, **559** (2013) 64–68.
27. R.D. Shannon, "Revised effective ionic radii and systematic studies of interatomic distances in halides and chalcogenides", *Acta Crystal. A*, **32** (1976) 751–767.
28. Y. Tomioka, T. Okuda, Y. Okimoto, R. Kumai, K. Kobayashi, "Magnetic and electronic properties of a single crystal of ordered double perovskite Sr_2FeMoO_6", *Phys. Rev. B*, **61** (2000) 422–427.
29. J.B. Goodenough, "Theory of the role of covalence in the perovskite-type manganites $[La_M(II)]MnO_3$", *Phys. Rev.*, **100** (1955) 564–573.
30. S.Y. Dan'kov, A.M. Tishin, V.K. Pecharsky, K.A. Gschneidner, "Magnetic phase transitions and the magnetothermal properties of gadolinium", *Phys. Rev. B*, **57** (1998) 3478–3490.
31. V.K. Pecharsky, K.A. Gschneidner, "Magnetocaloric effect and magnetic refrigeration", *J. Magn. Magn. Mater.*, **200** (1999) 44–56.
32. X. Bohigas, J. Tejada, E. del Barco, X.X. Zhang, M. Sales, "Tunable magnetocaloric effect in ceramic perovskites", *Appl. Phys. Lett.*, **73** (1998) 390–392.
33. Z.B. Guo, Y.W. Du, J.S. Zhu, H. Huang, W.P. Ding, D. Feng, "Large magnetic entropy change in perovskite-type manganese oxides", *Phys. Rev. Lett.*, **78** (1997) 1142–1145.
34. P.G. Radaelli, D.E. Cox, M. Marezio, S.W. Cheong, P.E. Schiffer, A.P. Ramirez, "Simultaneous structural, magnetic, and electronic transitions in $La_{1-x}Ca_xMnO_3$ with x = 0.25 and 0.50", *Phys. Rev. Lett.*, **75** (1995) 4488–4491.
35. K.H. Kim, J.Y. Gu, H.S. Choi, G.W. Park, T.W. Noh, "Frequency shifts of the internal phonon modes in $La_{0.7}Ca_{0.3}MnO_3$", *Phys. Rev. Lett.*, **77** (1996) 1877–1880.
36. T. Tang, K.M. Gu, Q.Q. Cao, D.H. Wang, S.Y. Zhang, Y.W. Du, "Magnetocaloric properties of Ag-substituted perovskitetype manganites", *J. Magn. Magn. Mater.*, **222** (2000) 110–114.
37. M.H. Phan, S.B. Tian, S.C. Yu, A.N. Ulyanov, "Magnetic and magnetocaloric properties of $La_{0.7}Ca_{0.3-x}Ba_xMnO_3$ compounds", *J. Magn. Magn. Mater.*, **256** (2003) 306–310.
38. Y. Sun, W. Tong, Y. H. Zhang, "Large magnetic entropy change above 300 K in $La_{0.7}Sr_{0.3}Mn_{0.9}Cr_{0.1}O_3$", *J. Magn. Magn. Mater.*, **232** (2001) 205–208.
39. M.A. Hamad, "Magnetocaloric effect in $Ge_{0.95}Mn_{0.05}$ Films", *J. Superconduct. Novel Magn.*, **26** (2013) 449–453.
40. M.A. Hamad, "Magnetocaloric effect in $La_{1-x}Cd_xMnO_3$", *J. Supercond. Nov. Magn.*, **26** (2013) 3459–3462.
41. M.A. Hamad, "Magnetocaloric effect in polycrystalline $Gd_{1-x}Ca_xBaCo_2O_{5.5}$", *Mater. Lett.*, **82** (2012) 181–183.